Macromolecular Journals

Plasma Processes and Polymers

ppap.201400194C

Full Paper

The properties of thin silica-like moisture barrier films roll-to-roll deposited on the polymeric web by AP-PECVD were investigated as function of the dynamic deposition rate and substrate temperature. The demonstrated WVTR barrier of $\approx 1.8 \times 10^{-3}$ $g \cdot m^{-2} \cdot day$ (at 40 °C, 90% RH) for 100 nm thick single layer silica-like film is comparable or better than the results obtained by low the pressure technology.

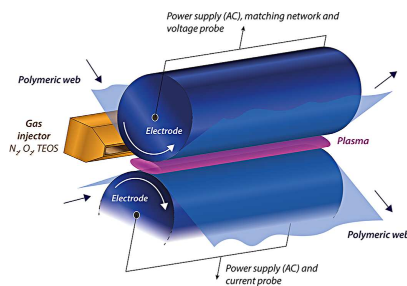

Towards Roll-to-Roll Deposition of High Quality Moisture Barrier Films on Polymers by Atmospheric Pressure Plasma Assisted Process

S. A. Starostin,* M. Creatore, J. B. Bouwstra, M. C. M. van de Sanden, H. W. de Vries

Plasma Process. Polym. **2014,** *11,* 000–000

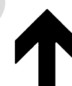

Early View Publication; these are NOT the final page numbers, use DOI for citation !!

UNCORRECTED PROOFS

ppap.201400194

Towards Roll-to-Roll Deposition of High Quality Moisture Barrier Films on Polymers by Atmospheric Pressure Plasma Assisted Process

Sergey A. Starostin,* Mariadriana Creatore, Jan B. Bouwstra, Mauritius C. M. van de Sanden, Hindrik W. de Vries

An atmospheric pressure dielectric barrier discharge (DBD) was applied for the deposition of silica-like moisture barrier films on polyethylene 2,6 naphthalate foil. The diffuse plasma was sustained between two cylindrical drum electrodes in N_2/O_2/Ar gas flow with the addition of tetraethyl orthosilicate. The chemical composition, morphology and water vapour transmission rate of the moisture permeation barrier layers were studied as a function of the dynamic deposition rate and substrate temperature. It was demonstrated that dense silica-like layers of 100 nm thick with a good permeation barrier of $\approx 1.8 \times 10^{-3}$ g · m^{-2} · day (at 40 °C, 90% RH), corresponding to three orders of magnitude barrier improvement with respect to the pristine polymer, can be deposited in an atmospheric pressure process.

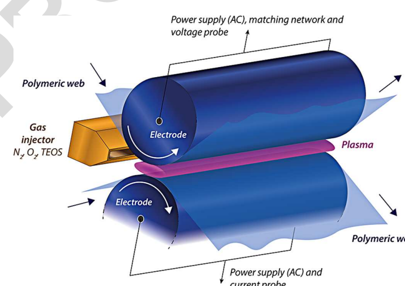

UNCORRECTED PROOFS

1. Introduction

Atmospheric pressure plasma enhanced chemical vapour deposition (AP-PECVD) of thin functional films has the potential to circumvent the limitations imposed by conventional low pressure deposition methods. These limitations are primarily related to the high costs and large footprint of vacuum equipment as well as the necessity to use batch processing or complex transfer chambers. Yet, the main question is whether atmospheric pressure deposition can lead to similar or even better thin film performance when compared to the well-established low pressure PECVD. At the same time from a scientific point of view there is a need to fill the existing knowledge gap between film properties and deposition mechanisms in atmospheric pressure plasma.

Deposition of thin transparent gas diffusion barrier films can be considered as one of the most challenging applications for PECVD technology, requiring low costs, large area compatibility and excellent layers in terms of uniformity, density and low defect level. The application field of these layers is very broad ranging from food, beverage and drug/medical-packaging towards more demanding applications, such as flexible solar cells or OLED displays.[1–3] For flexible electronic devices the main targets are to achieve prolonged life time stability (in order of several years) by limiting the water vapour transmission rate (WVTR) and oxygen transmission rate (OTR) through the encapsulating envelope.

While there is a large number of publications on low pressure deposited thin barrier films and their

Dr. S. A. Starostin, Prof. M. C. M. van de Sanden, Dr. H. W. de Vries
Dutch[Q1] Institute for Fundamental Energy Research (DIFFER), P.O. Box 1207, 3430 BE Nieuwegein, The Netherlands
E-mail: s.a.starostin@differ.nl
Dr. M. Creatore, Prof. M. C. M. van de Sanden
Plasma and Materials Processing Group, Department of Applied Physics, Eindhoven University of Technology, P.O. Box 513, 5600 MB Eindhoven, The Netherlands
Dr. J. B. Bouwstra
FUJIFILM Manufacturing Europe B.V, P.O. Box 90156, Tilburg, The Netherlands

© 2014 WILEY-VCH Verlag GmbH & Co. KGaA, Weinheim

Early View Publication; these are NOT the final page numbers, use DOI for citation !!

characterization much less is known in the field of gas diffusion barriers developed under atmospheric pressure.[4–14] The AP-PECVD processed oxygen barriers were studied in,[15–17] however, the performance of those films was not sufficiently optimized to be competitive with low pressure technology. In a prior article we have reported that by means of AP-PECVD it is possible to produce a thin single layer silica-like gas diffusion barrier on PEN foil with a WVTR $<5\ 10^{-3}\ g \cdot m^{-2} \cdot day^{-1}$ and OTR $<5\ 10^{-3}\ cm^3 \cdot m^{-2} \cdot day^{-1} \cdot bar^{-1}$, nevertheless, the dependency of barrier film properties on the deposition conditions was not addressed and discussed there.[18]

At atmospheric pressure the development of a plasma source suitable for the deposition of uniform high quality films compatible with processing at large area with a high throughput is a serious challenge from the scientific and technological point of view.

This research adopts the high current diffuse dielectric barrier discharge (DBD), which can be attributed to the glow-like discharge type.[19] The classical DBD is a common source of non-thermal plasma at atmospheric pressure.[20] This type of DBD (also known as corona discharge in industry) produces a filamentary plasma, having a strong spatial non-uniformity in power dissipation and plasma–chemical reaction rates.[20,21] The uncommon diffuse modes of the DBD identified as low current atmospheric pressure Townsend-like discharge (APTD) and high current atmospheric pressure glow-like discharge (APGD) were recently recognized as promising tools for plasma assisted deposition of high quality films.[22–24] The high current APGD mode is typically observed for a narrow parametric window of dissipated power densities, discharge frequencies and requiring gas mixtures strongly diluted by helium or argon.[23] However, we have already shown that smooth inorganic silica-like as well as organic carbon-rich films can be deposited in a diffuse glow-like discharge operating in cost-efficient nitrogen-based gas mixtures, or, even, using air as the process gas.[25]

A number of process parameters has a significant effect on the general properties of the PECVD synthesized barrier film such as chemical composition, morphology, film density and adhesion to the substrate. Some of these correlations were already discussed in selected publications from our group.[26–28] More general plasma chemical pathways of thin film deposition from organosilicon precursors in atmospheric pressure DBDs were investigated in.[29–31]

From the application point of view it is necessary to know how and why the barrier film quality depends on the reactor throughput. In the case of thin film deposition on a moving web the throughput is expressed by the dynamic deposition rate (DDR) value, defined as the product of film thickness and web transport speed. Another important characteristic for any kind of plasma–chemical process is the specific energy delivered per precursor molecule, or related to this, the Yasuda composite power parameter. This parameter is defined as the ratio between dissipated power and the product of monomer flow and monomer molecular weight.[32] The influence of Yasuda parameter on atmospheric pressure plasma-polymerization of HMDSO was recently Q2 studied.[33] In the case of fixed input power and complete precursor depletion in the plasma the variation in monomer flow will result in scaling of both DDR value and energy spent per monomer molecule. In[34] we already showed that the variation of specific energy dissipated in the discharge has a strong effect on both the refractive index and OTR value of the silica-like films. For the specific case study here under analysis, it is found that the rate of surface reactions and structure of the deposited film are strongly influenced by the substrate temperature.[17,35,36]

The novelty of the present work is the investigation of the atmospheric pressure barrier deposition process in a system closely compatible to industrial production demands. To enable such industrial roll-to-roll processing a cylindrical drum electrode configuration was implemented, while previous investigations were carried out for plane parallel electrodes.[17,25–28] The influence of two key parameters, namely dynamic deposition rate and substrate temperature was investigated comprehensively in relation to moisture barrier performance. The emphasis was put on highlighting and discussing the specific energy value required for the deposition of good performing barrier films at atmospheric pressure.

2. Experimental Section

The silica-like films were synthesized in a roll-to-roll PECVD reactor open to ambient air. The schematic view picture of the system is presented in Figure 1. The DBD was ignited between two cylindrical rotary drum electrodes with a radius of 120 mm, covered by optical grade thermally stabilized Polyethylene-2,6-naphthalate (PEN) foil 100 μm thick and 18 cm width (TEONEX Q65FA produced by Dupont Teijin Films). To enable precise temperature control the drum electrodes were equipped with a spiral tube affixed to the inner surface of the metal electrode shell. The heated liquid (oil) was pumped through the spiral tube to control the temperature of the drum electrode surface within ± 1 °C of the set value of the oil heater. The foil served two purposes, first, as the dielectric layer in the DBD arrangement and second, as the substrate for deposition. Both the top and bottom electrodes were equipped with independent roll-to-roll foil transport and tension control systems. The foil transport speed was varied from 50 mm/min to 300 mm/min. The effective discharge width was 15 cm and the smallest gaseous gap was 0.5 mm. For the investigated experimental conditions the characteristic discharge expansion length along the gas flow was typically 2 cm. However, the exact dimension of plasma expansion depends on the applied power, gas mixture and gas flow rate. The plasma was created using a high frequency

UNCORRECTED PROOFS

Plasma Process. Polym. 2014, DOI: 10.1002/ppap.201400194
© 2014 WILEY-VCH Verlag GmbH & Co. KGaA, Weinheim
DOI: 10.1002/ppap.201400194
Early View Publication; these are NOT the final page numbers, use DOI for citation !!

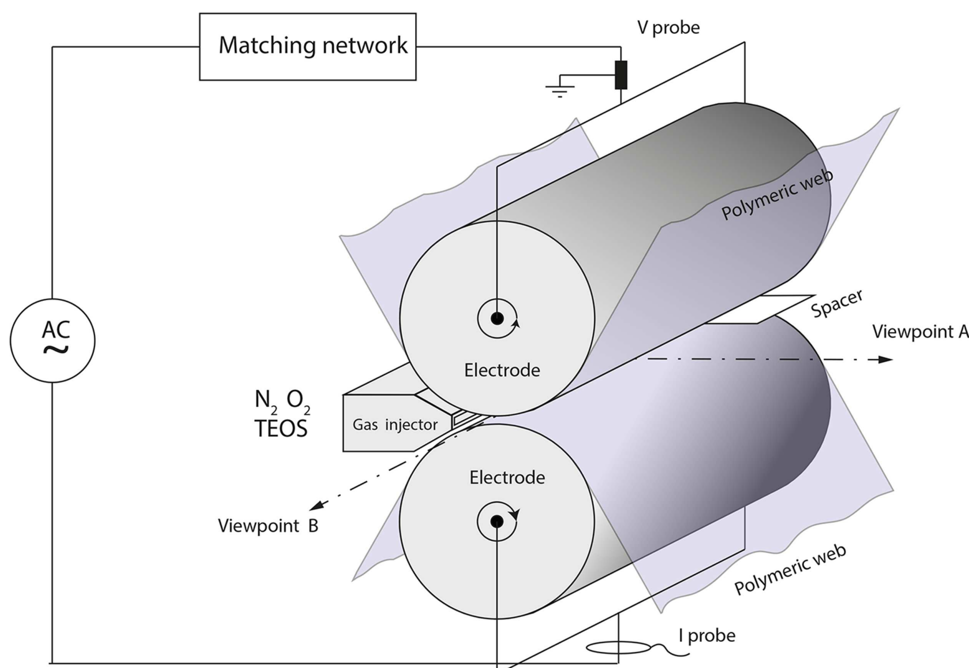

Figure 1. Schematic picture of the experimental setup.

generator from Seren Industrial Power Systems (L3001). The metal drum electrodes were connected to an external AC cirquit via carbon brush type electrical contacts. The operational frequency was tuned in the interval of 180–200 kHz to optimize forward power matching. The reactor was operating in the pulsed mode with a high voltage HV pulse duration of 800 μs and 90% duty cycle. The voltage amplitude between the electrodes was 2–3 kV. The reflected power was typically in the range 2–5% of the forward signal and was accounted for in the presented data. The power dissipated in the discharge was 575 W corresponding to approximately 19.2 W/cm^2 specific power density. The discharge current and voltage were measured by Pearson current monitor 4100 and Tektronix P6015A probe respectively. The *I*–*V* waveforms of the discharge are shown in Figure 2. It can be estimated that the peak current density averaged over treated surface area can reach about 170 mA/cm^2. This value is considerably higher than the typical Townsend-like discharge current densities which usually do not exceed 0.5–1.0 mA · cm^{-2}.[23] The instantaneous current densities can be even higher, because the discharge will form localized propagating ionization waves at nanosecond time scale.[19]

Tetraethylorthosilicate (TEOS), $Si(OC_2H_5)_4$, and oxygen were used as reactive gases, diluted in nitrogen carrier gas. For the present experimental arrangement approximately 70% of the supplied gas flow was passing the active plasma zone contributing to the deposition process. Part of the gas flow was lost via the narrow gap (≈100 μm) between gas injector and electrodes (see Figure 1). Due to its high vapour pressure at room temperature, the TEOS (Sigma–Aldrich, ≥99.0%) was injected via a controlled evaporation mixer (CEM) unit (Bronkhorst) where monomer vapours were mixed with 1 slm argon flow. The gas flow of nitrogen was 20 slm. The precursor and oxygen admixtures were simultaneously adjusted with fixed ratio of 4.5 10^{-3} in the range of 1.8 · 10^{-3}–10.8 · 10^{-3} slm and 0.4–2.4 slm respectively to govern the dynamic deposition rate in the interval of 10 – 60 nm · m · min^{-1}. All the gases were mixed in the buffer chamber before they were introduced into the plasma. For the studied conditions the reactor was operating in the complete precursor depletion mode. Precursor depletion was confirmed by the infrared absorption analysis of the exhaust gas in the long-path cell. It should be noted that the minor presence of argon in the gas mixture was not critical for the discharge properties or thin film synthesis, but based on the construction of the precursor injection system.

The temperature of the substrate during the deposition process was measured by an infrared camera, FLIR A320, from the effluent

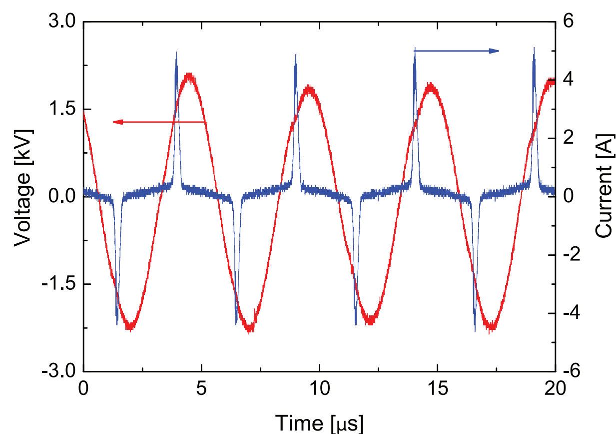

Figure 2. Voltage and current waveforms of the DBD during deposition process.

© 2014 WILEY-VCH Verlag GmbH & Co. KGaA, Weinheim

Early View Publication; these are NOT the final page numbers, use DOI for citation !!

side of the PECVD reactor indicated as viewpoint A in Figure 1. The infrared measurements were verified with a fibre optic thermal probe from OPTOcon FOTEMP in the absence of plasma for set values of electrode temperatures up to 100 °C.

The thickness of the films was determined using a variable angle spectroscopic ellipsometer (M-2000D, J.A.Woollam Inc.) in the wavelength range of 400–1000 nm. The employed optical model was composed out of three sub-layers: the polymer substrate, silica-like film and the surface roughness layer. The polymer and silica layers were modelled using the Cauchy dispersion function. The Bruggeman effective medium approximation was applied for the surface roughness layer. The optical model did not take into account the substrate anisotropy as previously done in.[34] X-ray photoelectron spectroscopy (XPS) was performed using Mg K_α X-ray source with a photon energy of 1253.6 eV (PHI 5500). Atomic force microscopy (AFM) measurements were carried out in the peak force tapping mode using Si tips with a radius of 6–8 nm (Bruker Dimension Icon). The captured AFM images were then processed using open source Gwyddion software for the surface profile analysis.[37] The RMS roughness of the untreated PEN substrate foil was 1.65 ± 0.03 nm. During the deposition process plasma uniformity was controlled by the Dalsa EC-11–05H40 sensitive array camera with 13 μs frame integration time. Visual and sensitive array camera observations of the discharge confirm the diffuse character and good uniformity of the plasma across the width of treated polymeric foil.[26]

Synthesized coatings were analysed by attenuated total reflection Fourier-transform infrared absorption spectrometry (ATR-FTIR) using a PerkinElmer Frontier instrument equipped with a single reflection Ge crystal ATR accessory. It should be noted that PEN substrate has strong absorption bands in the spectral region of 1000–1200 cm^{-1}, overlapping with the main absorption peaks of silica-like films. Therefore, for the purpose of absorption spectra analysis, the samples for ATR-FTIR were deposited on polyethylene terephthalate (PET) foil pre-coated with 1 μm thick polyvinylidene chloride (PVDC) layer. This simplifies the subtraction of the substrate absorption spectra because the PVDC layer prevents penetration of the evanescent wave into the underlying PET substrate and the PVDC layer has no strong absorption peaks in the regions of interest.

WVTR was measured using Technolox Deltaperm instrument (ASTM D 1434–82 (2003), sensitivity of $2\,10^{-4}\ g \cdot m^{-2} \cdot day^{-1}$) for the conditions of 40 °C, 90% RH unless stated otherwise. The area of tested samples was 50 cm^2. To reach stable transmission rate 50–100 hrs measurement time was required. During the mesaurement the WVTR value was recorded each minute. The average of the last 100 experimental points was presented as characteristic WVTR with the standard deviation being below 1%. The WVTR value of the pristine PEN substrate is 1.7 $g \cdot m^{-2} \cdot day^{-1}$.

The adhesion of deposited layers to the polymeric substrate was evaluated with a cross-cut tape adhesion test ISO 2409. For all films described in this publication no evidence of delamination was found after tape removal.

3. Results and Discussion

The variation of deposition rate provided by the change in precursor mass flow has a profound effect on the film morphology and chemical composition, as well as permeation properties. At the same time, for a fixed value of the discharge power in a precursor deficient regime, a variation in monomer flow defines the characteristic energy spent per precursor molecule. The dynamic deposition rate is largely determined by the specific reactor configuration such as active deposition length and the method of precursor injection, while the energy delivered per precursor molecule is a universal parameter.

The dependency of the WVTR value of the silica films on the dynamic deposition rate (DDR) is shown in Figure 3. The insert graph in Figure 3 presents how the WVTR is changing with the specific energy spent per deposited precursor molecule. The specific energy values were estimated from the dissipated power and the deposition rate assuming nearly stoichiometric amorphous silicon oxide with the density of 2.2. g/cm^3. The variation of DDR was provided by the variation in TEOS flow ($1.8 \cdot 10^{-3}$–$10.8 \cdot 10^{-3}$ slm), while the web speed was scaled (50–300 mm · min^{-1}) proportionally to the average deposition rate in order to deposit films at constant thickness of 100 nm. For the dynamic deposition rate calculation it should be taken into account that films are simultaneously synthesized on two substrate webs (see Figure 1). The oxygen flow rate (0.4–2.4 slm) was scaled with the TEOS flow rate, to keep a constant ratio between precursor and oxygen concentration. The substrate temperature measured with the infrared camera was 125 °C. For the DDR values of 10 nm · m · min^{-1} and 60 nm · m · min^{-1} the estimated energy spent per TEOS molecule is 6.5 keV/molecule and 1.1 keV/molecule, respectively. Figure 3 shows that an increase in the dynamic deposition rate corresponding to a decrease in the specific energy spent per TEOS molecule results in a steep rise in WVTR.

The deposition rate values averaged over the process length are 250 nm/min and 1500 nm/min for the DDR

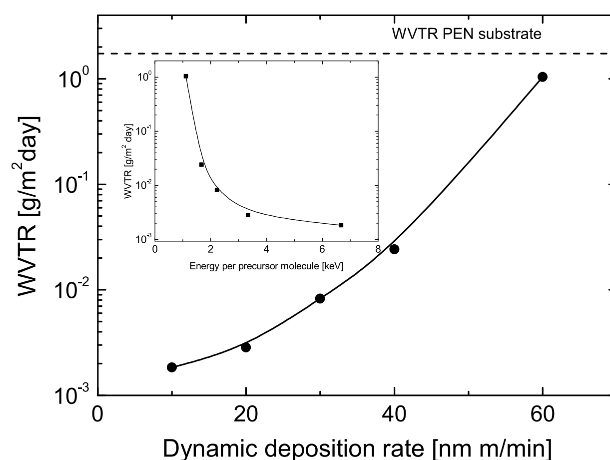

Figure 3. Dependency of WVTR value for 100 nm thick silica lm on the dynamic deposition rate. The insert graph shows how WVTR is changing with specic energy delivered per TEOS molecule.

UNCORRECTED PROOFS

© 2014 WILEY-VCH Verlag GmbH & Co. KGaA, Weinheim
DOI: 10.1002/ppap.201400194
Early View Publication; these are NOT the final page numbers, use DOI for citation !!

values of $10\,nm \cdot m \cdot min^{-1}$ and $60\,nm \cdot m \cdot min^{-1}$, respectively. Note that the maximum value of local deposition rate can be considerably higher due to the non-uniformity of the deposition rate profile along the gas flow induced by the precursor depletion.[38] For assessing the value of DDR and the system throughput, one should take into account that the plasma-active zone in the present experimental setup (≈2 cm) is relatively short and therefore the local deposition rate values for PECVD of dense inorganic films are rather high.

The film composition derived from the XPS analysis for dynamic deposition rate values of 10 and $60\,nm \cdot m \cdot min^{-1}$ is reported in Table 1. One can see that the film remains essentially inorganic for both extreme cases with the residual carbon content below the detection limit.

The variation in film composition and structure as a function of the dynamic deposition rate can be complemented by means of ATR-FTIR spectroscopy. For a comparative evaluation of the silica-like film quality several absorption bands are of special interest.[39,40] The peak related to Si—OH stretch vibrations in silanol is located at $930\,cm^{-1}$ and vibrations of —O—H groups in the 2800–$3600\,cm^{-1}$ region. The major absorption feature in the region of 1040–$1250\,cm^{-1}$ is corresponding to the asymmetric stretch vibrations of the Si—O—Si unit. This vibration consists of two overlapping modes: in-phase (AS1) and out of phase (AS2). In turn, each mode splits into transverse optical (TO) and longitudinal optical (LO) pairs.[41,42]

In Figure 4a we show how the infrared absorption spectra change in the region 750–$1300\,cm^{-1}$ with variation in dynamic deposition rate. This graph corresponds to the WVTR dependency on DDR for 575 W dissipated power as shown in Figure 3. Looking to the peak at $930\,cm^{-1}$ which is related to the Si—OH bonds, it can be concluded that more silanol is incorporated into the film as the DDR increases. At the same time the main absorption feature at $1060\,cm^{-1}$ which can be attributed to the in-phase asymmetric stretch of Si—O—Si (AS1) is sharpening and shifting towards higher wavenumbers. The shift is monotonic versus increase in DDR value, although for reasons of clarity in Figure 4a we show only the spectra corresponding to DDR of

Table 1. XPS compositional analysis results of the samples deposited at different substrate temperatures and dynamic deposition rates.

Substrate Temperature [°C]	Dynamic Deposition Rate [nm m/min]	Si [at. %]	O [at. %]	C [at. %]
82	20	33.3	66.4	0.2
125	10	33.5	65.8	0.3
125	60	30.7	69.1	0.1
140	20	32.0	67.3	0.3

$10\,nm \cdot m \cdot min^{-1}$ and $60\,nm \cdot m \cdot min^{-1}$. Generally it is assumed that both, a shift of the AS1 peak towards a value of $1078\,cm^{-1}$ (characteristic to thermal oxide) and a decrease in bandwidth are indicating silica-like film densification.[35,43,44] The observed opposite behaviour is rather unexpected but already reported in the literature. In[17] a similar shift of the AS1 peak to higher wavenumbers was well correlated with an increase in OTR for silica films. It was discussed in[17] that this behaviour can be related to the modification of Si—O bond environment, when the presence of Si—OH groups is shifting the oscillation of Si—O in AS1 peak to higher frequency. Comparable behaviour was observed by Pliskin[43] for the silica film produced by the electron beam evaporation after exposure to a humid environment. In the last case the peak at $930\,cm^{-1}$ attributed to the Si—O stretching vibration of strongly hydrogen bonded silanol Si—OH, was correlated with a pronounced decrease in bandwidth and blue shift of the AS1 feature. This observation was explained on the basis of silanol formation leading to strain relief in Si—O bonds as well as to less variability in the bond force constants. Therefore the shift to higher frequencies accompanied with a decrease in bandwidth can take place without densification if the density of silanol groups increases. On the other hand, it can be expected that the shift towards lower frequencies upon —OH groups reduction, observed in the present experiments, is non-monotonic and can be followed by the opposite blue shift upon further densification of the film.[44]

The broad absorption feature in the region of 2800–$3700\,cm^{-1}$ is attributed to the —O—H vibration. It can be considered as a superposition of 3 peaks with: 1) peak centered at $3350\,cm^{-1}$ attributed to OH in adsorbed water on the layer 2) peak centered at $3515\,cm^{-1}$ attributed to associated silanol groups and 3) peak centered at $3640\,cm^{-1}$ attributed to isolated silanol groups.[17,35,45] Figure 4b demonstrates the change in spectral feature at 2800–$3700\,cm^{-1}$ as a function of dynamic deposition rate. One can see that an increase in the deposition rate leads to an increase in silanol density both in associated and isolated states, pointing out again to a decrease mass density in the deposited layers. This trend supports the decrease in barrier properties as shown in Figure 3.

The change in surface morphology with increase in dynamic deposition rate from $10\,nm \cdot m \cdot min^{-1}$ to $60\,nm \cdot m \cdot min^{-1}$ is shown in Figure 5a, b which present the $2 \times 2\,\mu m^2$ AFM micrographs for 100 nm thick films. The WVTR performance for these layers was shown in Figure 3. In[27,28] we already studied the surface dynamics of the silica-like films grown by AP-PECVD process. Compared to our previous investigation the micrographs presented here are corresponding to the films deposited in the discharge between cylindrical drum electrodes at substantially higher dissipated power density.

UNCORRECTED PROOFS

© 2014 WILEY-VCH Verlag GmbH & Co. KGaA, Weinheim

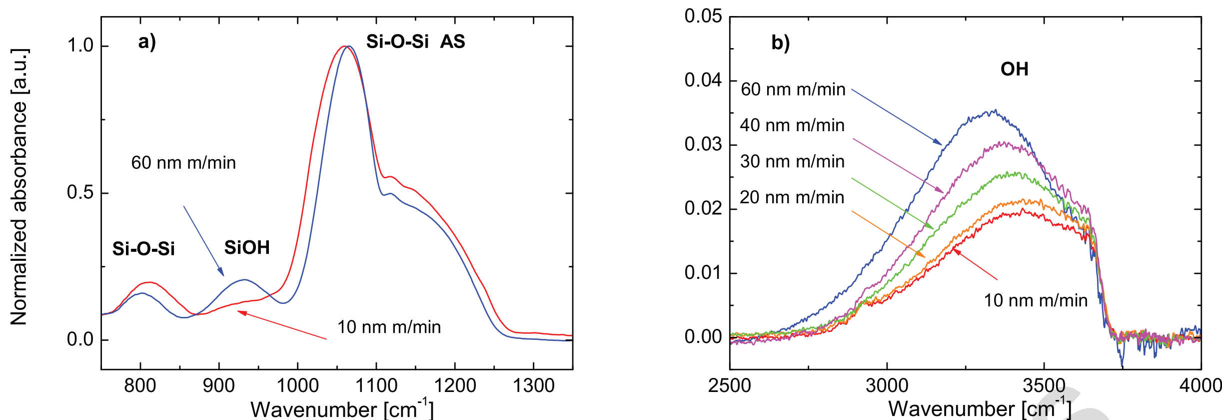

Figure 4. ATR-FTIR spectra of the silica-like lms synthesized at different dynamic deposition rates for a) 750–1350 cm^{-1} spectral region; b) 2500–4000 cm^{-1} spectral region.

UNCORRECTED PROOFS

Although the presence of surface features can be seen on both AFM scans in Figure 5a,b, the overall RMS roughness remains low (Rq = 1.7 nm) and comparable with the bare polymer (1.65 ± 0.03 nm). Nevertheless the number of small features is clearly growing as the deposition rate increases. This is a somewhat different behaviour compared to the morphologies that we observed earlier in[28] where carbon containing films were grown from hexamethyldisiloxane (HMDSO) precursor in the DBD process between plane-parallel electrodes, and a reduction of surface roughness was obtained with the deposition rate.

Figure 3 is indicating the specific energy in the order of a few keV, which needs to be delivered per precursor molecule in the gas discharge for synthesis of the good performing barrier films. At the same time the energy required for the direct scission of the C—O or Si—O bonds in TEOS monomer which is an obvious prerequisite for inorganic film formation is significantly lower: 4.0 eV–5.0 eV per bond, respectively.[29] From Figure 3 and Table 1 it can also be seen that inorganic films are produced for the entire studied range of specific energy, while barrier properties have a steep dependency on the specific energy. From the considerations discussed above it can be concluded that high specific energy values are required not merely for scission of the hydrocarbon groups, but mostly for the densification of the deposited layer. While densification of silica-like films via ion bombardment is a known process in low pressure PECVD (i.e.[46]), at atmospheric pressure one would expect that incident ions have only near thermal energies. However, a detailed numerical study indicates that in the cathode sheath region of the atmospheric pressure DBD discharge generated in air, the ion energy can reach up to 20 eV due to a substantial compression of the electric field. [47] In addition one should consider the energy delivered to the surface of the growing film by the ion-electron recombination, quenching of the vibrational and electronically excited states, UV irradiation and interaction with the radicals formed in plasma.

It should be emphasized that, regarding the energy budget required for deposition of dense silica-like film, the discharge mode with a high specific power density (≈20 $W \cdot cm^{-2}$) employed in the present work has clear advantages in terms of throughput and layer quality compared to the low current APTD-like discharge (0.5 $W \cdot cm^{-2}$).[17] Moreover, the mechanisms leading to the formation of energetic ions will be valid for glow-like discharge where significant field compression in the cathode fall region can be expected.[47] However, such a mechanism is not applicable to Townsend-like modes, where the electric field is practically unaffected by the volumetric charge.

The dependency of WVTR on film growth process temperature for a fixed value of the dissipated power of 575 W, DDR of 10 $nm \cdot m \cdot min^{-1}$ and film thickness of 100 nm is shown in Figure 6. The substrate temperature was adjusted by the variation of the circulating oil temperature within the range of 30–100 °C. The actual process temperature was in situ monitored by the infrared camera. Without plasma the measured substrate temperature was equal to the set value of the heater, however the plasma process introduces an additional heat source which induces a considerable temperature rise. For the given dissipated power of 575 W the surface temperature increase was typically 40–50 °C above the temperature of the circulating oil in the electrodes. In Figure 6 one can see that the WVTR dependency on the temperature has a minimum at approximately 120–130 °C. Remarkably this value is rather close to the glass transition temperature (T_g) of the polymeric PEN substrate which is ≈121 °C.[48] Moreover, similar WVTR values have been obtained on PET substrates (not shown here), having a considerably lower glass transition temperature of ≈78 °C.[48] It should be noted that not merely the value of the process temperature, but

Plasma Process. Polym. 2014, DOI: 10.1002/ppap.201400194
© 2014 WILEY-VCH Verlag GmbH & Co. KGaA, Weinheim
DOI: 10.1002/ppap.201400194
Early View Publication; these are NOT the final page numbers, use DOI for citation !!

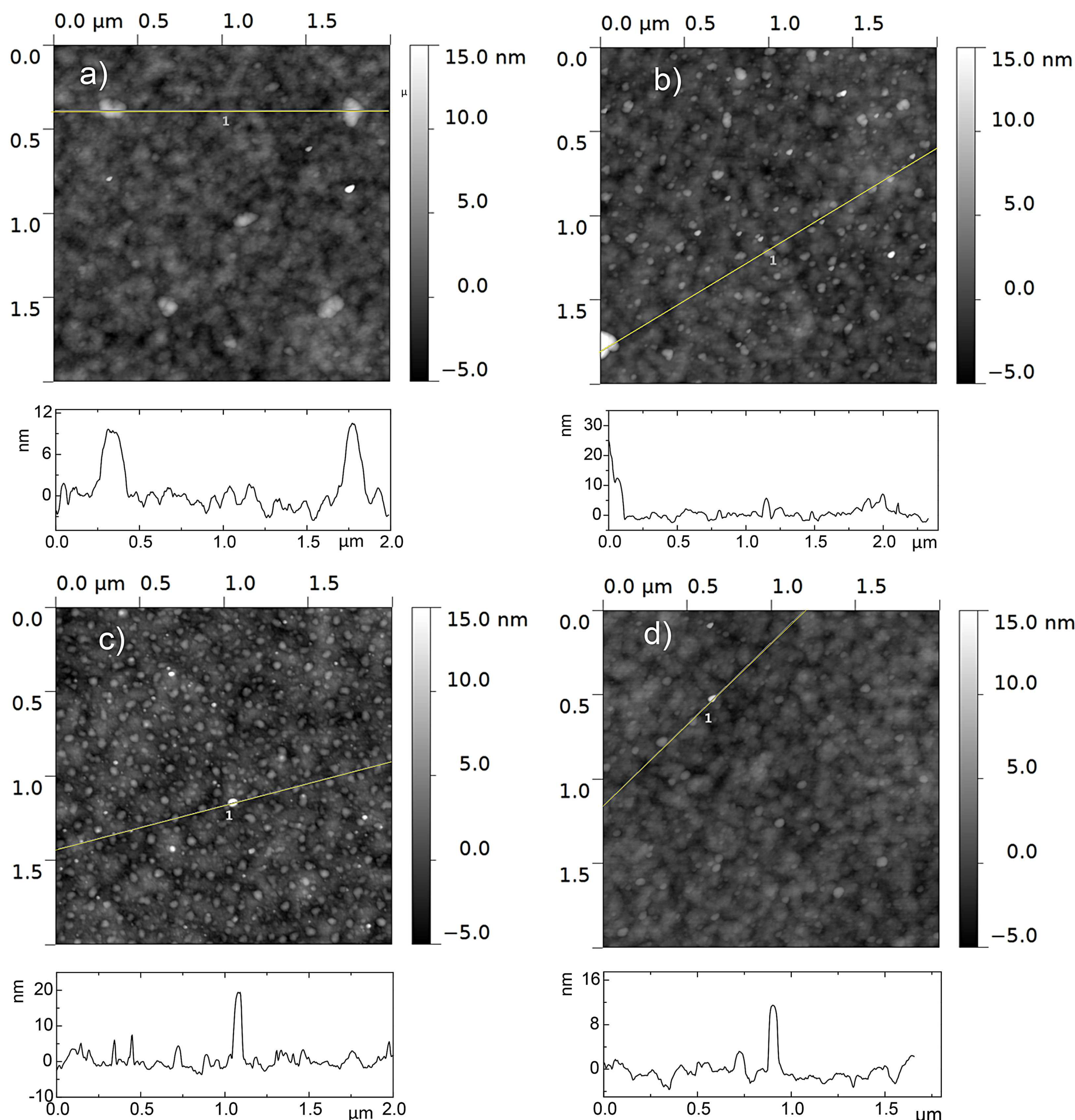

Figure 5. AFM micrographs and line proles of the 100 nm thick silica-like lm produced at different dynamic deposition rates (DDR) and substrate temperatures Ts a) DDR = 10 nm m/min, Ts = 125 °C, Rq = 1.7 ± 0.1 nm; b) DDR = 60 nm m/min, Ts = 125 °C, Rq = 1.7 ± 0.2 nm; c) DDR = 20 nm m/min, Ts = 82 °C, Rq = 1.7 ± 0.1nnm d) DDR = 20 nm m/min, Ts = 140 °C , Rq = 1.4 ± 0.1 nm.

also the residence time in the plasma is an important factor in the deposition process. For the experimental conditions presented in Figure 6, the residence time of the polymer in plasma was approximately 12 s. Generally, the dependency of WVTR on process temperature of silica-like films displays a similar trend as the OTR behaviour Q3reported.[17]

ATR-FTIR spectra of the films synthesized at different substrate temperatures corresponding to the WVTR data in Figure 6 are presented in Figure 7a,b. The variation in absorption spectra with substrate temperature as shown in Figure 7a,b is similar to the effect of dynamic deposition rate described above. Both, higher process temperature and lower deposition rate lead to a reduction of silanol groups in the film and a red shift of the peak related to the asymmetric stretch vibration of Si—O—Si. A qualitative interpretation of the Si—OH peak intensity by in situ ATR-FTIR spectra as a

© 2014 WILEY-VCH Verlag GmbH & Co. KGaA, Weinheim

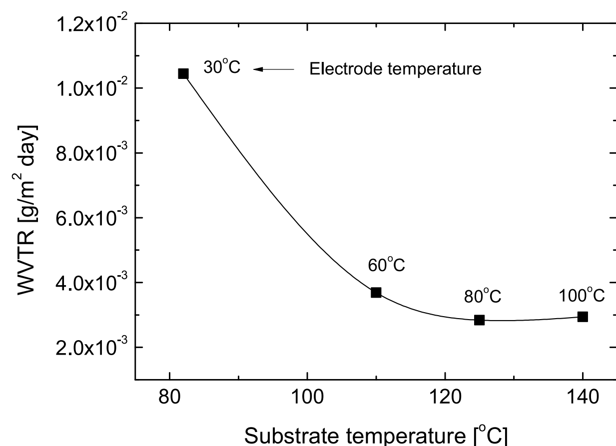

Figure 6. Dependency of the WVTR on the process temperature for 100 nm thick silica-like lms. The electrode temperature is indicated above the experimental points. The difference between electrode and substrate temperatures reflects the additional substrate heating by the discharge.

function of deposition rate and temperature was given by Deshmukh and Aydil for low pressure PECVD of silica-like films from TEOS.[35] In[35] Si—OH was considered as an intermediate deposition product, while silica network would be formed by surface reactions of the adjacent Si—OH groups and subsequent water release. The removal rate of silanol species would increase with surface temperature. Given the time required for the removal reaction, an increase in deposition rate (i.e. by increase in TEOS flow) can lead to conditions where the Si—OH has no time to react and will be ̈buried£ in the growing film. Comparing the trends seen in Figure 7a,b with barrier performance in Figure 6 one can note that although the presence of the silanol groups is still reducing for temperatures above 130 °C or deposition rates below 10 nm · m · min^{-1} the barrier performance does not improve significantly. It can be argued that under these conditions the water permeation is limited by the local defect density (either substrate-related pinholes or environmental dust). One can also note that although the intensities of —OH related infrared absorption peaks are comparable in Figure 4 and Figure 7 for the case of 1) dynamic deposition rate of 60 nm · m · min^{-1} and substrate temperature of 125 °C and 2) dynamic deposition rate of 20 nm · m · min^{-1} and substrate temperature of 82 °C, the difference in WVTR between those two cases is almost two orders of magnitude (see Figure 3 and 6). Therefore, solely monitoring the —OH group density in the deposited film cannot give direct quantitative indication of absolute WVTR value.

AFM micrographs of the silica-like films deposited at 82 °C and 140 °C (Figure 5c,d) show a substantial change in morphology with the deposition temperature. Low temperature results in the appearance of multiple blister-like features although the RMS roughness remains relatively low (Rq = 1.7 ± 0.1 nm). At higher temperature the RMS roughness slightly reduces (Rq = 1.4 ± 0.1) as well as the film surface has apparently less features. A qualitatively similar behaviour of the film topology as a function of deposition temperature was observed in[17] for the silica-like layers deposited in a Townsend discharge.

It is interesting to compare the WVTR data for 100 nm thick film obtained in the present work (i.e. see Figure 3: 1.8 10^{-3} g · m^{-2}day^{-1} at 40 °C, 90% RH) with the data presented in the literature for single layer silica like films. The WVTR reported in[14] for a 100 nm thick film produced by MW plasma assisted process (measured at 25 °C, 85% RH) is ≈2 10^{-2} g · m^{-2}day^{-1}. For the alternative low pressure PECVD technique assisted by Penning discharge[12] the moisture barrier for 200 nm thick silica-like film, roll-to-roll deposited on PEN substrate, was 0.71 g · m^{-2} day^{-1} (50 °C, 100% RH).

UNCORRECTED PROOFS

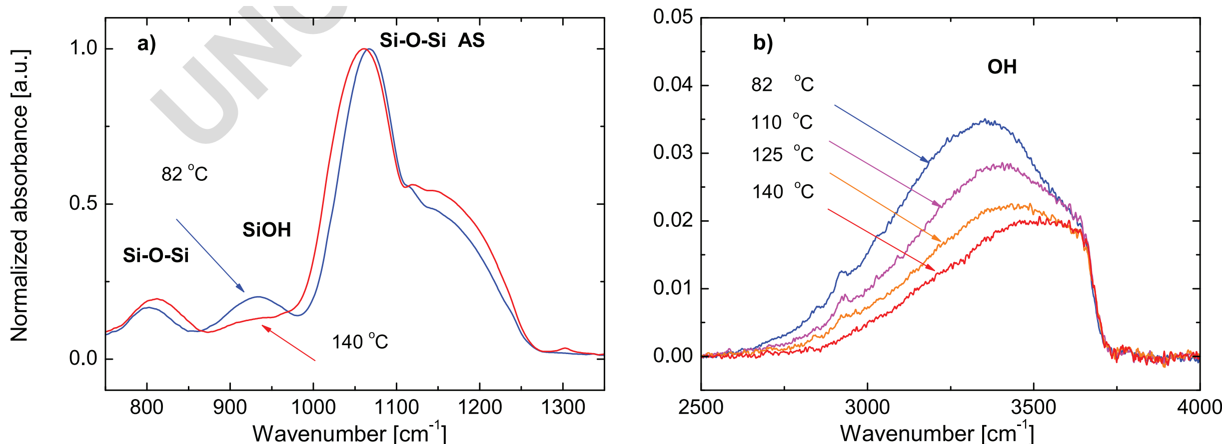

Figure 7. ATR-FTIR spectra of the silica-like lms synthesized at different substrate temperatures for a) 750–1350 cm^{-1} spectral region b) 2500–4000 cm^{-1} spectral region.

Plasma Process. Polym. **2014,** DOI: 10.1002/ppap.201400194
© 2014 WILEY-VCH Verlag GmbH & Co. KGaA, Weinheim
DOI: 10.1002/ppap.201400194
Early View Publication; these are NOT the final page numbers, use DOI for citation !!

From the examples above one can conclude that AP-PECVD is capable of producing films with similar or better performance compared to low pressure technology. It is necessary to emphasize that except prior publication from our group,[18] to our knowledge, the possibility to deposit good performing moisture barrier films at atmospheric pressure was not reported before.

4. Conclusion

The present work demonstrates the significant potential of the high current atmospheric pressure DBD for deposition of thin inorganic moisture barriers films on polymeric webs in an open air roll-to-roll process. The gas discharge was sustained between cylindrical electrodes in a cost effective gas mixture of $N_2/Ar/O_2$/TEOS, these conditions are compatible to industrial roll-to-roll processing. The discharge plasma has a diffuse appearance and results in uniform, smooth and well adherent coatings with good effective moisture barrier performance in the range of 10^{-3} $g \cdot m^{-2} day^{-1}$ (40 °C, 90% RH). This result is typically better than a single layer silica-like barrier films deposited at low pressure PECVD.[12,14] Both, dynamic deposition rate and polymeric substrate temperature were shown to be important parameters to control moisture barrier properties. Although the films remain inorganic for the whole studied range of deposition rates and process temperatures, a strong and correlated variation in the density of silanol groups and moisture permeation properties was observed. Deposition rate and substrate temperature also have a pronounced effect on the thin film morphology, studied by AFM. In the investigated system reduction in deposition rate and increase in temperature results in smoother films with less surface features, although for the whole studied parametric range roughness of a 100 nm thick film remains comparable to the pristine polymeric substrate (< 2 nm). It was shown that the formation of dense inorganic silica-like barrier layer is characterized by the specific energy of a few keV per monomer molecule dissipated in plasma. The relatively high energy budget may indicate additional densification mechanisms as discussed in literature and has a good synergy with the high specific power density of the APGD-like discharge mode employed for deposition.

Acknowledgements: The presented study was performed in the frame of LIFE12 ENV_NL_000718 "Green plasma process technology for manufacturing of flexible electronics" project and industrial partnership program between Dutch Foundation for Fundamental Research on Matter (FOM) and FUJIFILM Europe B.V. The authors are grateful to Patrick Marcus from Bruker Company for AFM analysis of the AP-PECVD samples. The authors are also grateful to dr. Kirsten Schiffmann (Fraunhofer IST) for the XPS measurements. The research of M.C. has been funded by the Netherlands Organization for Scientific Research (NWO, Aspasia program).

Received: October 3, 2014; Revised: November 17, 2014; Accepted: November 18, 2014;DOI: 10.1002/ppap.201400194

Keywords: atmospheric pressure glow discharges (APGD); dielectric barrier discharges; roll-to-roll reactors; gas diffusion barrier films; water-vapour permeability

[1] J. Lewis, *Mater. Today* **2006**, *9*, 38.
[2] J. S. Park, H. Chae, H. K. Chung, S. I. Lee, *Semicond. Sci. Technol.* **2011**, *26*, 034001.
[3] N. Grossiord, J. M. Kroon, R. Andriessen, P. W. M. Blom, *Org. Electron.* **2012**, *13*, 432.
[4] H. Chatham, *Surf. Coat. Technol.* **1996**, *78*, 1.
[5] J. D. Affinito, M. E. Gross, C. A. Coronado, G. L. Graff, I. N. Greenwell, P. M. Martin, *Thin Solid Films* **1996**, *290–291*, 62.
[6] A. G. Erlat, R. J. Spontak, R. P. Clarke, T. C. Robinson, P. D. Haaland, Y. Tropsha, N. G. Harvey, E. A. Vogler, *J. Phys. Chem. B* **1999**, *103*, 6047.
[7] A. S. D. Sobrinho, M. Latreche, G. Czeremuszkin, J. E. Klemberg-Sapieha, M. R. Wertheimer, *J. Vac. Sci. Technol. A* **1998**, *16*, 3190.
[8] M. Creatore, F. Palumbo, R. d'Agostino, P. Fayet, *Surf. Coat. Technol.* **2001**, *142*, 163.
[9] A. Gruniger, A. Bieder, A. Sonnenfeld, P. N. von Rohr, U. Muller, R. Hauert, *Surf. Coat. Technol.* **2006**, *200*, 4564.
[10] E. Langereis, M. Creatore, S. B. Heil, M. C. van de Sanden, W. M. Kessels, *Appl. Phys. Lett.* **2006**, *89*, 08.
[11] P. F. Carcia, R. S. McLean, M. H. Reilly, M. D. Groner, S. M. George, *Appl. Phys. Lett.* **2006**, *89*, 03.
[12] D. G. Howells, B. M. Henry, J. Madocks, H. E. Assender, *Thin Solid Films* **2007**, *516*, 3081.
[13] S. Steves, B. Ozkaya, C.-N. Liu, O. Ozcan, N. Bibinov, G. Grundmeier, P. Awakowicz, *J. Phys. D: Appl. Phys.* **2013**, *46*, 084013.
[14] A. M. Coclite, F. De Luca, K. K. Gleason, *J. Vac. Sci. Technol. A* **2012**, *30*, 061502.
[15] B. L. O. Neill, L.-O. Hare, S. R. Leadley, A. J. Goodwin, *Chem. Vapor Depos.* **2005**, *11*, 477.
[16] P. Scopece, A. Viaro, R. Sulcis, I. Kulyk, A. Patelli, M. Guglielmi, *Plasma Process. Polym.* **2009**, *6*, S705.
[17] J. Petersen, J. Bardon, A. Dinia, D. Ruch, N. Gherardi, *ACS Appl. Mater. Interfaces* **2012**, *4*, 5872.
[18] P. Antony Premkumar, S. A. Starostin, M. Creatore, H. de Vries, R. M. J. Paffen, M. C. M. Koenraad, *Plasma Process. Polym.* **2010**, *7*, 635.
[19] S. A. Starostin, P. Antony Premkumar, M. Creatore, E. M. van Veldhuizen, H. de Vries, R. M. J. Paffen, M. C. M. van de Sanden, *Plasma Sources Sci. Technol.* **2009**, *18*, 045021.
[20] U. Kogelschatz, *Plasma Chem. Plasma Process.* **2003**, *23*, 1.
[21] H.-E. Wagner, R. Brandenburg, K. V. Kozlov, A. Sonnenfeld, P. Michel, J. F. Behnke, *Vacuum* **2003**, *71*, 417.
[22] S. Kanazava, M. Kogoma, T. Moriwaki, S. Okazaki, *J. Phys. D: Appl. Phys.* **1988**, *21*, 838.
[23] F. Massines, N. Gherardi, N. Naude, P. Segur, *Eur. Phys. J. Appl. Phys.* **2009**, *47*, 22805.
[24] F. Massines, C. Sarra-Bournet, F. Fanelli, N. Naude, N. Gherardi, *Plasma Process. Polym.* **2012**, *9*, 1041.

UNCORRECTED PROOFS

© 2014 WILEY-VCH Verlag GmbH & Co. KGaA, Weinheim

[25] S. A. Starostin, P. Antony Premkumar, M. Creatore, H. de Vries, R. M. J. Paffen, M. C. M. van de Sanden, *Appl. Phys. Lett.* **2010**, *96*, 061502.
[26] S. Starostine, E. Aldea, H. de Vries, M. Creatore, M. C. M. van de Sanden, *Plasma Process. Polym.* **2007**, *4*, S440.
[27] P. Antony Premkumar, S. A. Starostin, H. de Vries, M. Creatore, P. M. Koenraad, W. A. MacDonald, M. C. M. van de Sanden, *Plasma Process Polym.* **2012**, *9*, 1194.
[28] P. Antony Premkumar, S. A. Starostin, H. de Vries, M. Creatore, P. M. Koenraad, M. C. M. van de Sanden, *Plasma Process Polym.* **2013**, *10*, 313.
[29] A. Sonnefeld, T. M. Tun, L. Zajickova, K. V. Kozlov, H.-E. Wagner, J. F. Behnke, R. Hippler, *Plasmas Polymers* **2001**, *4*, 237.
[30] F. Fanelli, S. Lovascio, R. d'Agostino, F. Fracassi, *Plasma Process. Polym.* **2012**, *9*, 1132.
[31] R. Reuter, K. Rugner, D. Ellerweg, T. de los Arcos, A. von Keudell, J. Benedikt, *Plasma Process. Polym.* **2012**, *9*, 1116.
[32] H. K. Yasuda, *Plasma Polymerization*, Academic Press Inc, Orlando **1985**.
[33] R. Morent, N. De Geyter, T. Jacobs, S. Van Vlierberghe, P. Dubruel, C. Leys, E. Schacht, *Plasma Process. Polym.* **2009**, *6*, S537.
[34] G. Aresta, P. Antony Premkumar, S. A. Starostin, H. de Vries, M. C. M. van de Sanden, M. Creatore, *Plasma Process. Polym.* **2010**, *7*, 766.
[35] S. C. Deshmukh, E. S. Aydil, *J. Vac. Sci. Technol.* **1995**, *13*, 2355.
[36] D. Trunec, L. Zajickova, V. Bursikova, F. Studnicka, P. Stahel, V. Prysiazhnyi, V. Perina, J. Houdkova, Z. Navratil, D. Franta, *J. Phys. D: Appl. Phys.* **2010**, *43*, 225403.
[37] D. Necas, P. Klapetek, *Cent. Eur. J. Phys.* **2012**, *10*, 181. (www.gwyddion.net).
[38] P. Antony Premkumar, S. A. Starostin, H. de Vries, R. M. J. Paffen, M. Creatore, T. J. Eijkemans, P. M. Koenraad, M. C. M. van de Sanden, *Plasma Process. Polym.* **2009**, *6*, 693.
[39] D. R. Anderson, *Analysis of Silicones*, Wiley, New York **1974**.
[40] P. J. Launer, *Silicon Compounds Register and Review*, Petrarch Systems, Bristol **1987**.
[41] I. P. Lisovskii, V. G. Litovchenko, V. G. Lozinskii, G. I. Steblovskii, *Thin Solid Films* **1992**, *213*, 164.
[42] C. T. Kirk, *Phys. Rev. B* **1988**, *38*, 1255.
[43] W. A. Pliskin, *J. Vac. Sci. Technol.* **1977**, *14*, 1064.
[44] P. Innocenzi, *J. Non-Cryst. Solids* **2003**, *316*, 309–319.
[45] A. Goullet, C. Vallée, A. Granier, G. Turban, *J. Vac. Sci. Technol. A* **2000**, *18*, 2452.
[46] A. Milella, M. Creatore, M. A. Blaw, M. C. M. van de Sanden, *Plasma Process. Polym.* **2007**, *4*, 621.
[47] N. Yu., M. Babaeva, Kushner, *Plasma Sources Sci. Technol.* **2011**, *20*, 035017.
[48] W. A. MacDonald, M. K. Looney, D. MacKerron, R. Eveson, R. Adam, K. Hashimoto, K. Rakos, *J. SID* **2007**, *15/12*, 1075.

Q1: Author: Please confirm that the given names (red) and surnames/family names (green) have been identified correctly.
Q2: Author: The influence of Yasuda......was recently studied. This sentence has been reworded for clarity. Please check and confirm it is correct.
Q3: Author: Generally, the......behaviour reported. This sentence has been reworded for clarity. Please check and confirm it is correct.

UNCORRECTED PROOFS

Plasma Process. Polym. **2014,** DOI: 10.1002/ppap.201400194
© 2014 WILEY-VCH Verlag GmbH & Co. KGaA, Weinheim
DOI: 10.1002/ppap.201400194
Early View Publication; these are NOT the final page numbers, use DOI for citation !!

Plasma Processes and Polymers

Reprint order form 2014

Editorial office:
Wiley-VCH
Plasma Processes and Polymers
Boschstrasse 12, 69469 Weinheim
Germany

Tel.: +49 (0) 6201 606 – 581 or 238
Fax: +49 (0) 6201 606 – 510
E-mail: plasma@wiley-vch.de

http://www.plasma-polymers.org

Short DOI: ppap.____________________

Please send me and bill me for

☐ no. of **Reprints** via ☐ airmail (+ 25 Euro) ☐ surface mail

Please send me and bill me for a

☐ **high-resolution PDF file** (330 Euro).

My e-mail address:

____

Please note: It is not permitted to present the PDF file on the internet or on company homepages

Information regarding VAT
Please note that from German sales tax point of view, the charge for **Reprints, Issues or Posters** is considered as **"supply of goods"** and therefore, in general, such delivery is a subject to German sales tax. However, this regulation has no impact on customers located outside of the European Union. Deliveries to customers outside the Community are automatically tax-exempt. Deliveries within the Community to institutional customers outside of Germany are exempted from the German tax (VAT) only if the customer provides the supplier with his/her VAT number. The VAT number (value added tax identification number) is a tax registration number used in the countries of the European Union to identify corporate entities doing business there. It starts with a country code (e.g. FR for France, GB for Great Britain) and follows by numbers.

Cover Posters

Posters are available of all the published covers and frontispieces in two sizes

☐ DinA2 42 x 60 cm/ 17 x 24in (one copy: **39 Euro**)

☐ DinA1 60 x 84 cm/ 24 x 33in (one copy: **49 Euro**)

Postage for shipping posters overseas by airmail:
+ 25 Euro

Postage for shipping posters within Europe by surface mail:
+ 15 Euro

Mail reprints / posters to:

____
____
____
____
____

Invoice address:

____
____
____
____
____

VAT no.: ________________________
(Institutes / companies in EU countries only)

Purchase Order No.: ________________

Credit Card Payment:

VISA, MasterCard, AMERICAN EXPRESS
Please use the Credit Card Token Generator located at the website below to create a token for secure payment. The token will be used instead of your credit card number.

Credit Card Token Generator:
https://www.wiley-vch.de/editorial_production/index.php

Please transfer your token number to the space below.

Credit Card Token Number

Price list for reprints (The prices include mailing and handling charges. All Wiley-VCH prices are exclusive of VAT)

No. of pages	Price (in Euro) for orders of					
	50 copies	100 copies	150 copies	200 copies	300 copies	500 copies
1-4	345	395	425	445	548	752
5-8	490	573	608	636	784	1077
9-12	640	739	786	824	1016	1396
13-16	780	900	958	1004	1237	1701
17-20	930	1070	1138	1196	1489	2022
for every additional 4 pages	147	169	175	188	231	315

★ **Special Offer** ★ If you order 200 or more reprints you will get a PDF file for half price.

Wiley-VCH Verlag GmbH & Co. KGaA; Location of the Company: Weinheim;
Chairman of the Supervisory Board: Stephen Michael Smith,
Trade Register: Mannheim, HRB 432833, General Partner: John Wiley & Sons GmbH,
Location: Weinheim, Trade Register Mannheim, HRB 432296,
Managing Directors: Bijan Ghawami, Dr. Jon Walmsley

WILEY-VCH

USING e-ANNOTATION TOOLS FOR ELECTRONIC PROOF CORRECTION

Required software to e-Annotate PDFs: Adobe Acrobat Professional or Adobe Reader (version 7.0 or above). (Note that this document uses screenshots from Adobe Reader X)
The latest version of Acrobat Reader can be downloaded for free at: http://get.adobe.com/uk/reader/

Once you have Acrobat Reader open on your computer, click on the Comment tab at the right of the toolbar:

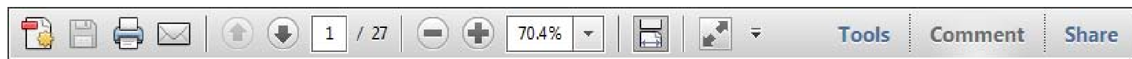

This will open up a panel down the right side of the document. The majority of tools you will use for annotating your proof will be in the Annotations section, pictured opposite. We've picked out some of these tools below:

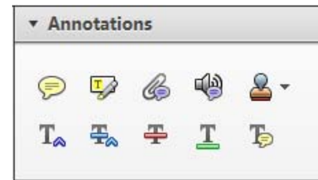

1. Replace (Ins) Tool – for replacing text.

Strikes a line through text and opens up a text box where replacement text can be entered.

How to use it

- Highlight a word or sentence.
- Click on the Replace (Ins) icon in the Annotations section.
- Type the replacement text into the blue box that appears.

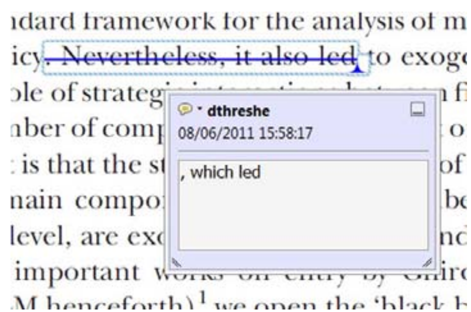

2. Strikethrough (Del) Tool – for deleting text.

Strikes a red line through text that is to be deleted.

How to use it

- Highlight a word or sentence.
- Click on the Strikethrough (Del) icon in the Annotations section.

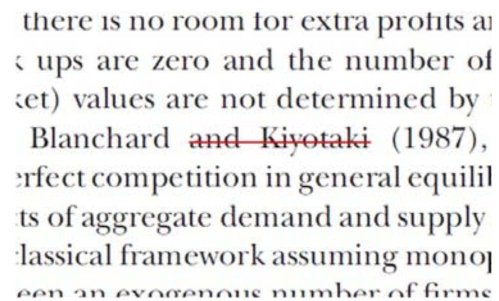

3. Add note to text Tool – for highlighting a section to be changed to bold or italic.

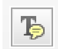

Highlights text in yellow and opens up a text box where comments can be entered.

How to use it

- Highlight the relevant section of text.
- Click on the Add note to text icon in the Annotations section.
- Type instruction on what should be changed regarding the text into the yellow box that appears.

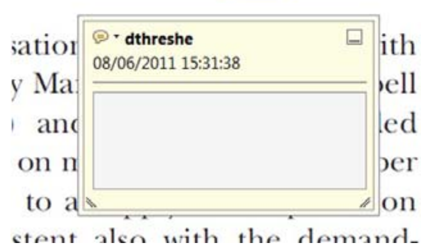

4. Add sticky note Tool – for making notes at specific points in the text.

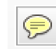

Marks a point in the proof where a comment needs to be highlighted.

How to use it

- Click on the Add sticky note icon in the Annotations section.
- Click at the point in the proof where the comment should be inserted.
- Type the comment into the yellow box that appears.

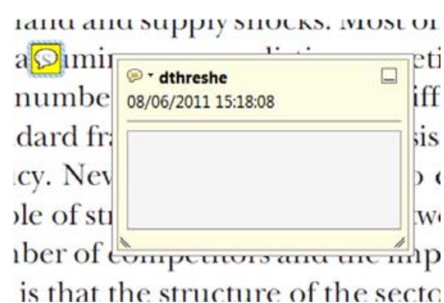

USING e-ANNOTATION TOOLS FOR ELECTRONIC PROOF CORRECTION

5. Attach File Tool – for inserting large amounts of text or replacement figures.

Inserts an icon linking to the attached file in the appropriate pace in the text.

How to use it

- Click on the Attach File icon in the Annotations section.
- Click on the proof to where you'd like the attached file to be linked.
- Select the file to be attached from your computer or network.
- Select the colour and type of icon that will appear in the proof. Click OK.

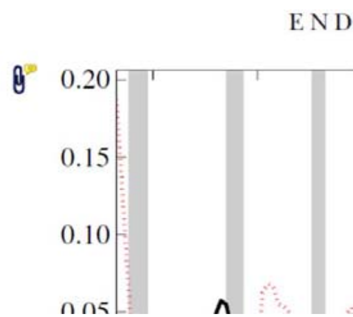

6. Add stamp Tool – for approving a proof if no corrections are required.

Inserts a selected stamp onto an appropriate place in the proof.

How to use it

- Click on the Add stamp icon in the Annotations section.
- Select the stamp you want to use. (The Approved stamp is usually available directly in the menu that appears).
- Click on the proof where you'd like the stamp to appear. (Where a proof is to be approved as it is, this would normally be on the first page).

7. Drawing Markups Tools – for drawing shapes, lines and freeform annotations on proofs and commenting on these marks.

Allows shapes, lines and freeform annotations to be drawn on proofs and for comment to be made on these marks..

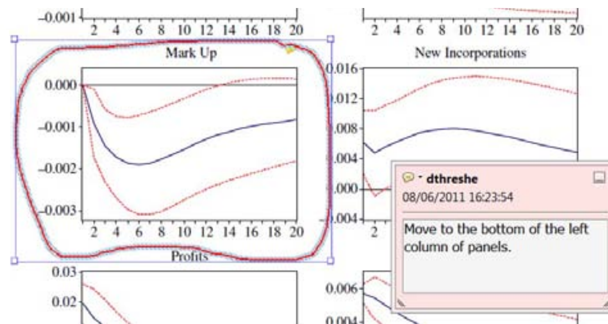

How to use it

- Click on one of the shapes in the Drawing Markups section.
- Click on the proof at the relevant point and draw the selected shape with the cursor.
- To add a comment to the drawn shape, move the cursor over the shape until an arrowhead appears.
- Double click on the shape and type any text in the red box that appears.

For further information on how to annotate proofs, click on the Help menu to reveal a list of further options: